NASA Technical Memorandum 89017

Radiometric Responsivity Determination for Feature Identification and Location Experiment (FILE) Flown on Space Shuttle Mission 41-G

R. Gale Wilson, Richard E. Davis,
Robert E. Wright, Jr., W. E. Sivertson, Jr.,
and Gordon F. Bullock

DECEMBER 1986

NASA

NASA Technical Memorandum 89017

Radiometric Responsivity Determination for Feature Identification and Location Experiment (FILE) Flown on Space Shuttle Mission 41-G

R. Gale Wilson, Richard E. Davis,
Robert E. Wright, Jr., W. E. Sivertson, Jr.,
and Gordon F. Bullock

Langley Research Center
Hampton, Virginia

National Aeronautics
and Space Administration

**Scientific and Technical
Information Branch**

1986

The use of trademarks or names of manufacturers in this report is for accurate reporting and does not constitute an official endorsement, either expressed or implied, of such products or manufacturers by the National Aeronautics and Space Administration.

Summary

A procedure was developed to obtain the radiometric (radiance) responsivity of the Feature Identification and Location Experiment (FILE) instrument in preparation for its flight on Space Shuttle Mission 41-G (November 1984). This instrument was designed to obtain Earth feature radiance data in spectral bands centered at 0.65 μm and 0.85 μm, along with corroborative color and color-infrared photographs, and to collect data to evaluate a technique for in-orbit autonomous classification of the Earth's primary features. The calibration process incorporated both solar radiance measurements and radiative transfer model predictions in estimating expected radiance inputs to the FILE on the Shuttle. The measured data are compared with the model predictions, and the differences observed are discussed. Application of the calibration procedure to the FILE over an 18-month period indicated a constant responsivity characteristic. This report documents the calibration procedure and the associated radiometric measurements and predictions that were part of the instrument preparation for flight.

Introduction

The Feature Identification and Location Experiment (FILE) flew on Shuttle Flight STS-2 (OSTA-1 payload) in 1981 and Flight 41-G (OSTA-3 payload) in 1984. The FILE experiment was designed to evaluate a two-channel spectral classification technique for autonomous classification of the Earth's primary features as described for the earlier flight in references 1 and 2. The radiometric responsivity of the instrument was defined through preflight calibration followed by postflight verification. Since there is no recognized standard or prescribed method for performing a radiometric calibration of an instrument such as the FILE, this report was written as a detailed documentation of the procedure used and of the preflight and postflight calibration measurements. The calibration approach is described after the following brief review of the FILE experiment.

FILE Experiment Description

Figure 1 is a sketch of the FILE system assembly. The instrument incorporates the following components: two charge-coupled device (CCD) cameras, one equipped with a narrow bandpass interference filter in the red part of the visible spectrum (fig. 2) and the other with a similar filter to pass a near-infrared (IR) band of radiation (fig. 3); two 70-mm film cameras, one equipped with color film and the other with color-IR film; a camera electronics unit; a buffer memory; and two tape recorders. Figure 4 is a sketch of the imaging lens in the FILE CCD cameras (D. O. Industries, Inc., 10.6-mm focal length). Figure 5 shows the field of view (FOV) of each camera for its 3- by 4-mm CCD sensor located at the back focal plane of one of these lenses. The FILE incorporated an optics assembly (fig. 6) to allow removal or installation of the filters and imaging lenses without disturbing the boresight settings of the CCD cameras.

The outputs of the CCD cameras (100- by 100-pixel sensor arrays) are converted from analog-to-digital form in the camera electronics unit, temporarily stored in the buffer unit, and then transferred to the tape recorders. The recorded digital data represent relative spectral radiance of Earth features, as measured by the two boresighted CCD cameras. The instrument (refs. 1 and 2) provides in-orbit classification of the Earth's features by using programmed information, including the Earth's spectral radiance, the solar zenith angle, and the instrument's spectral radiance responsivity. The features are classified as vegetation; water; bare land; or clouds, snow, and ice as a group. The color and color-IR photographs provide supporting (i.e., "ground-truth") data for postflight analysis of the classification accuracy and for algorithm optimization studies.

Instrument Calibration Approach

The approach to calibration of the instrument emphasized maximizing signal-to-noise ratio for each camera through internal camera gain settings and through choosing camera apertures to provide near full-scale output (without saturation) of each camera for the maximum-radiance feature (clouds). The procedural steps are summarized as follows:

1. Obtain a reference reflectance (calibration) target suitable for field use; the target also serves as a cloud simulator
2. Measure spectrophotometrically the reflectance (in the FILE instrument passbands) of the target and qualify it as a diffuse reflector
3. Obtain a radiometer suitable for use as a FILE reference instrument for measurement of radiance from the calibration target
4. Adapt the reference radiometer to measure spectral radiance in the FILE instrument passbands
5. Establish a method and laboratory apparatus to verify the initial (manufacturer) calibration of the reference radiometer and to verify radiometric stability of the radiometer from the preflight through the postflight period
6. From ground measurements of solar radiance reflected by the calibration target and from predictions based on an atmospheric radiative transfer

computer model, estimate the maximum cloud radiance to be sensed by the FILE instrument in orbit

7. Adjust the electronic gain of each FILE instrument CCD camera to provide just-under-saturation output of its analog-to-digital converter to allow maximum signal-to-noise ratio

8. Illuminate the reflectance panel in a laboratory setting with high-intensity flood lamps to simulate the cloud-radiance input to FILE

9. With both FILE and the radiometer viewing the reflectance panel, equip the FILE instrument with lenses of suitable apertures to provide full-scale response for the two spectral channels

10. Determine the spectral radiance responsivity for each FILE instrument camera in $V/mW\text{-}cm^{-2}\text{-}sr^{-1}\text{-}\mu m$

The reference standard of radiance used to verify the radiometer calibration was a tungsten-strip lamp, calibrated and supplied by the National Bureau of Standards (NBS). A target area of the lamp filament, for which radiance data were supplied by NBS, was imaged onto a pinhole which served as the "near small source" for the Jones method (refs. 3 and 4 and also described later in the present paper) of verifying the radiometer calibration.

Transmission functions of the interference filters were checked frequently during the preflight and postflight periods to assure that there was no physical degradation. Postflight measurements of the spectral responsivity (FILE passbands) of the reference radiometer were made for comparison with the preflight measurements to verify constancy of the radiometer responsivity characteristics. Application of the calibration procedures to FILE before and after flight indicated constant responsivity characteristics of the FILE instrument throughout a 1.5-year period of testing and evaluation.

Instrument Spectral Responsivity Determination

Definition of Spectral Bandpasses

The FILE design provides Earth feature classification based on the radiance level measured in a narrow band (fig. 2) centered at 0.65 μm and on the ratio of radiance measured in this band to that measured in a similarly narrow band (fig. 3) centered at 0.85 μm (refs. 1 and 2). Filters (Ditric Optics, Inc., 3-cavity construction) designed to retard degradation by moisture were used; their spectral responses were monitored by repeated spectrophotometric measurements of their transmission properties, starting from the time the filters were purchased and continuing through a postflight instrument evaluation. Spectrally matching filters were simultaneously purchased for a calibration radiometer to be used in radiometrically calibrating FILE. All filters were specified to be manufactured just before delivery, with delivery time arranged to be 8 weeks before assembly of the instrument for flight. Figures 2 and 3, respectively, present transmission functions for the 0.65- and 0.85-μm filters both for FILE and the calibration radiometer. There was no significant change in the measured FILE or radiometer filter transmission functions between the time of receipt of the filters from the manufacturer and the postflight evaluation (about 1.5 years). The filter specifications and selection process resulted in a suitable match between the center wavelength and bandpass characteristics of the 0.65- and 0.85-μm filters, as well as suitable matching between radiometer and FILE filters for each passband.

Description of the Calibration Radiometer

The radiometer/photometer system used for calibration measurements, an EG&G Model 550, included a multipurpose detector designed for measuring several radiometric and photometric quantities. For the measurements reported herein, the radiometer was operated in its radiance-measurement mode and provided readout in units of $\mu W/cm^2\text{-}sr$. The radiometer incorporates a silicon photovoltaic detector with a circular sensitive area of about 1.0 cm^2 and has provision to compensate for unwanted background radiation. The radiometer includes a spectral-response flattening filter, which is a multilayer subtractive filter that is computer designed to correct the silicon detector response to a constant sensitivity (± 7 percent) over the spectral range from 475 nm to 975 nm. This filter and the manufacturer-supplied 2.5° field stop (optional) are mounted directly over the silicon detector as shown in figure 7(a). The holder for the narrow passband filter (FILE passband) slides directly over the radiometer lens barrel and locks the filter flat against a lighttight seal on the end of the lens barrel. In the configuration used with the FILE work, the radiometer field of view was limited to 2.5° full angle to ease constraints on the operating distance of the radiometer from the reflectance calibration target and on the required area of uniform illumination of the target (important for indoor calibration of FILE with artificial illumination).

Bench Tests on Calibration Radiometer

The primary measurement of the FILE instrument is spectral radiance. The method chosen for

determining the responsivity of FILE was to measure with FILE a known spectral radiance reflected from a reference reflectance target, as determined with the calibration radiometer located beside FILE. This method of determining the responsivity of the FILE instrument is described in the literature (refs. 3 through 5) as the "near extended-source calibration," in which the source completely fills both the aperture and field of view of the instrument.

The method used to perform verification tests on the calibration radiometer is referred to in the literature as the "Jones method" (near small-source method) of calibration. The Jones method avoids the difficulty of providing an extended source of radiance with solar radiance levels in the bands of interest. A source that is small compared with the area of the radiometer aperture is placed close to that aperture in a position where it will irradiate the field stop of the instrument uniformly. The radiance responsivity of the instrument in V/mW-cm^{-2}-sr^{-1}, or similar units, then is (ref. 3, p. 9)

$$R_N = \frac{V}{N} = \frac{V}{N_s}\frac{A}{A_s}$$

where

$\frac{V}{N}$ expected voltage output of radiometer per unit of radiance if calibration were done with an extended source

$\frac{V}{N_s}$ measured voltage output of radiometer per unit of radiance from near small source (Jones method)

$\frac{A}{A_s}$ ratio of area of radiometer aperture (entrance pupil) to area of the small source

The test setup used to verify the reference radiometer calibration and constancy of the calibration with time is sketched in figure 7(a). The uniform radiance from a small target area (0.6- by 0.8-mm rectangle in fig. 7(b)) near the center of the standard lamp tungsten-strip filament is provided by NBS as lamp calibration data, for specified wavelengths, for the lamp operated at a designated current (General Electric P60 lamp operated at 39.200 A). For the 0.65- and the 0.85-μm center wavelengths, the standard lamp target radiances for the small target area, linearly interpolated over the bandpasses, are

$$N(0.65) = 13.45 \text{ W/cm}^2\text{-}\mu\text{m-sr}$$

$$N(0.85) = 21.15 \text{ W/cm}^2\text{-}\mu\text{m-sr}$$

The spectral radiances of the NBS-calibrated tungsten lamp were converted into in-band radiances, transmitted by the respective FILE narrowband filters, by multiplying each calibrated spectral radiance by an equivalent rectangular passband determined from the measured transmissions (figs. 2 and 3). The rectangular passband was determined by dividing the integrated (transmission-wavelength-interval product) areas under the transmission curves by unity transmission.

A relay lens (fig. 7(a)) located two focal distances f away from the lamp filament and an equal distance from a pinhole, produces a unit magnification image of the lamp filament onto the pinhole. The pinhole size was chosen (fig. 7(b)) to make the pinhole area nearly equal to the calibrated (target) area of the lamp filament for which the NBS radiance data were applicable, and the pinhole secondary source became the Jones method near small source. Because the Jones method requires the ratio of the radiometer aperture area to the radiance source area, both of these areas must be determined accurately. The pinhole diameter was measured with a Unitron TMS-2006 microscope. The entrance pupil diameter of the radiometer was determined from the manufacturer's drawings and specifications and was confirmed by direct measurement. The resultant ratio (A/A_s = (42 mm)^2/(0.77 mm)^2 = 2975) is not expected to be in error by more than 2 percent.

Table 1 compares the measured radiances (setup of fig. 7) of the standard lamp, for the two bandpasses, with the furnished NBS calibration data for the lamp for those bandpasses. The calibration data in the first and second columns of the table represent the standard lamp radiances in the equivalent ideal rectangular bandpasses (figs. 2 and 3), and in the third and fourth columns are listed the corresponding measured values for those bandpasses, including corrections for the relay lens attenuation (fig. 7). For each spectral passband the error in the radiance measurement is calculated as the percentage error in the measurement as compared with the calibrated radiance of the standard lamp. The percentage errors in the lamp radiance measurements lie within the 7-percent radiometric accuracy specification of the radiometer manufacturer. Therefore, the standard lamp spectral radiance measurements reported here are consistent with the manufacturer's radiance calibration on the instrument, which was done by an entirely different procedure. From table 1 it is seen that there was good repeatability for the two sets of measurements, made about 1 year apart.

Experimental and Analytical Solar Radiance Studies

Reflectance reference (calibration target). The EG&G Model 550 radiometer, with the appropriate narrow passband filter, was used to determine the reflectance reference (porcelain panel) spectral radiance and simultaneously the FILE CCD camera responsivity in volts per unit spectral radiance, as both the FILE and the calibration radiometer viewed the illuminated panel. The reflectance reference panel serving as a calibration target was a 1- by 1-m flat sheet of Armco Univit steel obtained from Vincent Brass and Aluminum Company and coated with a white porcelain enamel by Hanson Porcelain Company, Inc. In the laboratory the target was illuminated with high-intensity photofloods, to obtain solar radiance levels for the two passbands for setting the CCD camera dynamic ranges. The radiance dynamic ranges expected to be sensed by FILE in orbit were determined from the adjustment (as described later) of ground measurements of direct and indirect (diffuse) solar radiance reflected from the calibration target, made with the EG&G calibration radiometer equipped with the narrow passband filters. As noted, the passbands of the reference radiometer filters were matched to the ones in the FILE cameras. These solar measurements were made atop a horizontal roof about 10 m above ground level to reduce background obstruction (e.g., trees) of the indirect radiation.

The porcelain panel was obtained for use as a reflectance reference after discussions with NBS. Porcelain-enameled surfaces containing TiO_2 pigment, with the enamel baked on at an elevated temperature, are highly reflective, scratch resistant, and soil resistant (easily cleaned). Such surfaces are widely used in products of the illumination industry, and are used by NBS to make reference standard reflectance samples for use in spectrophotometry. Spectrophotometric measurements on samples (5 by 5 cm) removed from one edge of the porcelain-enameled sheet showed that the reflectance is 0.83 over the 0.65-μm passband and is 0.81 over the 0.85-μm passband. Spectrophotometric measurements of diffuse reflectance compared with measurements of diffuse-plus-specular reflectance indicated a specular component of 4 or 5 percent. The spectrophotometric reflectance (calibration target) and transmission (narrow bandpass filters) measurement procedures applied in the FILE calibration are described in the appendix.

Reference solar radiance measurements. Measurements of the total spectral radiance (direct solar plus diffuse) reflected from the porcelain panel were made with the calibration radiometer, equipped with bandpass filters, on two cloud-free, low humidity days during the hours of peak Sun elevation in November 1983 and February 1984. The solar zenith angles at the Langley Research Center, Hampton, Va., for the November and February measurements were 62°–63° and 53°–54°, respectively. The values of solar radiance measured (averaged) were 43.7 mW/cm^2-sr-μm for the 0.65-μm passband and 32.0 mW/cm^2-sr-μm for the 0.85-μm passband. The reflectance panel was maintained perpendicular to the direction of the Sun for all the measurements by nulling the shadow of a rod clamped perpendicularly to the panel. The radiometer readings were made 1.5 to 2 m from the panel and from view angles off normal (25°–35°) to avoid shadowing the panel and to avoid the specular component of reflection.

Prediction of solar radiance by computer model. In conjunction with the solar reflectance measurements on the porcelain panel, predictions of the reflected total radiance from the panel were made as checks on the measured radiances (roof top) and to obtain predictions of radiance levels expected to be sensed in Shuttle orbit. The measured reflectance of the panel was an input to the radiative transfer model used to make these predictions. The analytical computational program used was one obtained from the Environmental Research Institute of Michigan (ERIM) and was based on Turner's (refs. 6 and 7) radiative transfer model for the Sun-atmosphere system. The radiative transfer model was also used to calculate the expected values of solar radiance reflected from clouds viewed from orbit, based on cloud reflectance values of 0.70 in the 0.65-μm band and 0.69 in the 0.85-μm band. The radiative transfer model required as input the reflectance of the background surrounding the cloud target. The background reflectance used (table 2) was an averaged reflectance for all the major features, i.e., vegetation, bare land, water, and clouds. The reflectance data used as input to the computer radiative transfer model were based on a literature study and summaries reported in references 8 and 9. The reflectance data are consistent with a recent compilation of representative literature data (ref. 10).

The radiative transfer model predictions for the porcelain panel radiance ("observed" on the ground) at the FILE center-band wavelengths as a function of solar zenith angle, for a representative range of meteorological visibilities (related to aerosol content or haziness), are shown in figure 8. Similar predictions for clouds ("observed" from satellite altitude) are shown in figure 9. Since clouds were the major Earth feature with the highest radiance to be sensed

by FILE (for FILE classification purposes, clouds, snow, and ice are considered as a group) and the porcelain panel served as an approximate cloud simulator, it was useful to compare the predicted cloud radiance with the predicted panel radiance for the ranges of solar zenith angle and visibility studied. Figures 10 and 11, for the 0.65- and 0.85-μm wavelengths, respectively, show the ratio of the predicted radiance of clouds sensed at satellite altitudes to the predicted radiance of the porcelain panel sensed on the ground. It is seen that this ratio is nearly independent of solar zenith angle and varies over a range from about 0.65 to 0.80 for the range of visibility studied (8 to 48 km). These comparative radiance predictions for clouds and the porcelain panel serve to indicate that we should expect cloud radiance as seen by FILE on the Shuttle to be 65 to 80 percent of that reflected from the solar panel, as observed on the ground. We take 75 percent as a representative number for both passbands and for medium-to-high visibilities.

Atmospheric absorption and scattering effects within the FILE passbands are low. The radiative transfer model assumes Lambertian target and background reflectances. Consequently, for a target with a reflectance high enough that the target radiance is predominantly made up of the direct-beam radiance from the target instead of scattered radiance in the atmospheric path between the target and sensor, the variation in the radiance is essentially a function of the zenith angle. (This condition holds for the more nonhazy atmospheres and for target reflectances of 0.3 to 0.4 or greater. On the other hand, for targets of very low reflectance, haze can have a more marked effect.) The expected quasi-cosine behavior is exhibited in figures 8 and 9.

The solar radiance measurements on the porcelain panel, reported earlier, were made with the panel perpendicular to the direction of the Sun. The model-predicted radiances to which the measurements were compared are those for solar zenith angles between 55° and 65°. The meteorological visibility during the observations was estimated at 24 km. Figure 8 presents the radiance predicted for a horizontal surface, having the same reflectivity as the porcelain panel, viewed at a nadir angle equal to the solar zenith angle by an instrument with the Sun behind it. Since the model as implemented only applies to horizontal surfaces, the calculated radiance was divided by the cosine of the zenith angle to correct, to first order, the radiance values to those for a panel perpendicular to the Sun. When this correction was done for a zenith angle of 60°, radiances of 38.0 mW/cm^2-sr-μm at 0.65 μm and 25.2 mW/cm^2-sr-μm at 0.85 μm resulted. These values are both lower than the respective measured values of 43.7 and 32.0 mW/cm^2-sr-μm. This discrepancy between predicted and measured values is not completely understood but is believed to arise from two causes that are both related to the fact that the model only applies to horizontal surfaces: (1) The inclined panel reflecting surface intercepts some radiation diffusely reflected from the background surface (concrete-gravel coating) and (2) the panel, oriented perpendicular to the Sun, views a brighter circumsolar sky radiation field than does a horizontal panel viewing the whole sky. Reference 11, for example, presents a calculation of the sky radiance field.

Both of these phenomena, if taken into account in the model, would act to increase the model radiance values over those calculated, leading to better agreement with the observations. Reference 12 treats the reflected radiation contribution analytically, and the ERIM radiative transfer model gives values for the sky radiance in any direction. Spectral radiance estimates (predictions) for the tilted panel were made based on calculated estimates of (1) reflected direct radiance from the Sun, (2) reflected sky radiance, and (3) radiance reflected from the background. A background (roof) reflectance estimate of 0.6 and a solar zenith angle of 60° were used in the calculations. Average sky-radiance estimates of 25 mW/cm^2-sr-μm at 0.65 μm and 15 mW/cm^2-sr-μm at 0.85 μm were used. These calculations resulted in predictions of radiance that agreed with measured values to within 2 percent at 0.65 μm and 7 percent at 0.85 μm. These differences are acceptable, in view of the limited accuracy of the radiance measurements and in view of the fact that differences between radiative transfer model predictions and experimental measurement results continue to be a subject of active investigation (e.g., ref. 13). Reference 14 presents a detailed investigation of the relative contributions of the direct-solar, diffuse-sky, and background-reflectance-dependent components of irradiance incident upon a target surface in a field environment.

Estimation of FILE radiance inputs. To derive an estimate of cloud radiance expected to be sensed by FILE on the Space Shuttle, based on measured radiance on the porcelain panel and the modeling results, we multiplied the measured panel radiance by the ratio of predicted cloud radiance to predicted panel radiance and by a further factor to account for the applicable solar zenith angle. The zenith angle, however, is a variable with the Shuttle orbits. The range of solar zenith angles observed during a Shuttle orbit depends on the inclination of the Shuttle and the season. Our best estimate of a representative angle for the mission was 24°. After

the spectral radiances measured on the porcelain panel were multiplied by the two factors 0.75 (ratio of predicted cloud radiance to predicted porcelain panel radiance) and 0.91 (i.e., $\cos 24°$), the resultant best-estimate values of cloud radiance input to FILE on Shuttle were 29.8 mW/cm^2-sr-μm (43.7 by 0.75 by 0.91) for the 0.65-μm band and 21.8 mW/cm^2-sr-μm (32.0 by 0.75 by 0.91) for the 0.85-μm band.

Final Calibration of FILE

Optics settings. To provide a range of F-numbers (ratio of focal length to diameter of lens) from which to choose in the final calibration steps with the FILE instrument, we obtained pairs of identical lenses with F-numbers ranging from F/2.0 to F/8.0, in increments of 1/2 F/stop. A 1/2 F/stop difference accommodates a 25-percent radiance difference. The 10.6-mm-focal-length lens (fig. 4) was designed for good imaging quality for angles up to 15° off axis.

To provide maximum signal-to-noise ratio, the electronic gain of each FILE CCD camera was adjusted to provide just-under-saturation output of its analog-to-digital converter. Then, by an iterative procedure, as described subsequently, we selected lenses with F-numbers to provide full-scale responses for radiance inputs corresponding to those predicted for clouds (as seen by FILE from the Shuttle). Illuminating the porcelain reflectance panel with high-intensity photofloods produced an extended and repeatable source of radiance. With the reference radiometer and FILE both viewing the panel, the radiometer measured the radiance from the panel as we varied the lighting geometry to simulate the expected cloud radiance (from the Shuttle), first for the 0.65-μm camera. With that radiance level established, the 0.65-μm camera was fitted with a lens of suitable F-number to produce a full-scale response of the FILE (within the tolerance of the F-number selections available). Then this procedure was repeated for the 0.85-μm camera. The photoflood illumination used did not produce a uniform radiance from the porcelain surface. Therefore, the photofloods were arranged to produce a broad radiance peak whose shape was observed on the video display of the FILE camera and whose extent was within the radiometer 2.5° field of view.

After installation of the appropriate lenses, the cameras were boresighted by observing video outputs of their imagery for a suitably designed target placed distant from the cameras and by then locking them in their aligned positions with set-screw adjustments. Earlier, the overall uniformity of response of the CCD cameras had been verified in a larger-aperture configuration, at a lower (uniform) illumination level. After the final lens installations, we checked the linearity (table 3) of response by placing neutral density filters in front of the cameras to attenuate the (cloud-simulation-level) radiances.

FILE spectral responsivity. After selecting the lenses (F-numbers) for FILE, the instrument spectral responsivity was determined for each camera by dividing the voltage output of the camera by the best-estimate value of cloud radiance input to FILE on the Shuttle, presented earlier at the end of the section, "Estimation of FILE radiance inputs." The input data and responsivities finally determined for the instrument before the Shuttle 41-G flight are given in table 4. The spectral responsivities of the two cameras are somewhat different. An effective flat spectral response for the instrument can be obtained by applying a gain factor to the 0.65-μm camera voltage output. The gain factor is essentially the ratio of the 0.85-μm camera responsivity to the 0.65-μm camera responsivity. A further small iteration on the gain factor accounts for the fact that the selection of the 5.7 F-number lens provided 96 percent of full-scale output for the 0.65-μm camera, whereas it provided 92 percent of full-scale output for the 0.85-μm camera. The proper gain factor G to be applied to (multiplied by) the 0.65-μm camera output to produce results that would have been expected from a flat-response system, then, is (see table 4)

$$G_{0.65} = \left(\frac{R_{0.85}}{R_{0.65}}\right)\left(\frac{0.92}{0.96}\right) = 1.26$$

Concluding Remarks

The Feature Identification and Location Experiment (FILE), designed to classify Earth features from narrow-band spectral data centered at 0.65 μm and at 0.85 μm, flew on Shuttle flights STS-2 (1981) and 41-G (1984). The outputs of charge-coupled device (CCD) cameras equipped with interference filters for these two bands were converted from analog-to-digital form and recorded on magnetic tape for on-ground data processing and analysis, along with the analysis of corresponding color and color-infrared photographic data, and along with the analysis of results of real-time (in-orbit) classification based on an algorithm programmed into the instrument. Details have been presented of an approach to calibrating the instrument that emphasizes maximizing signal-to-noise ratio for each camera through internal camera gain settings and through choosing camera apertures to provide near full-scale

output (without saturation) of each camera for the maximum-radiance feature (clouds).

The calibration procedure was based on establishing in the laboratory radiance levels in the two spectral bands representing the best estimates of cloud radiance expected to be sensed by the FILE in Shuttle orbit and setting the CCD camera apertures to provide near-saturation camera outputs for those radiance levels. A commercial reference (calibration) radiometer was obtained for defining the radiance levels used in making the optical settings on the FILE. The spectral radiance responsivity of the FILE was determined by observing a reflectance reference panel with both the FILE and the calibration radiometer while the panel was illuminated at the maximum levels expected to be sensed by the instrument in the Shuttle mission. A test setup (based on a slight modification of the Jones calibration method) was assembled to verify the manufacturer's settings on the calibration radiometer and to recheck the radiometer's calibration throughout the period of preparation for the Shuttle mission and during the postmission recalibration of the FILE. Transmission functions of the interference filters were continuously monitored from preflight to postflight to assure that there was no physical degradation.

The calibration process incorporated both solar radiance measurements and radiative transfer model predictions in estimating expected radiance inputs to the FILE on the Shuttle. The measured data were compared with the model predictions and the differences observed were discussed. Application of the calibration procedure to FILE over a 1.5-year period indicated constant responsivity characteristics throughout this period of testing and evaluation.

NASA Langley Research Center
Hampton, VA 23665-5225
November 5, 1986

Appendix

Spectrophotometric Measurements for FILE Calibration

A Perkin-Elmer Model 330 spectrophotometer was used for all cited FILE calibration spectral measurements. A 60-mm-diameter integrating sphere accessory, Perkin-Elmer part H210-2101, was installed for the calibration target reflectance measurements. Data were acquired and processed with a Perkin-Elmer Model 3600 data station via PECDS-II and IF320 software. Reflectance measurements were referenced to the NBS Standard Reference Material (SRM) 2019A (white diffuser) by manual corrections to the reflectance of the working reference material, pressed aluminum oxide. The specifications of the manufacturer on this spectrophotometer in the specular transmission mode are as follows: wavelength accuracy in the ultraviolet-to-visible range, ±0.2 nm for 15°–25°C; wavelength repeatability, ±0.1 nm; photometric accuracy in the range of 350–878 nm, ±0.3 percent transmission; photometric repeatability, ±0.1 percent transmission.

The calibration target reflectance was measured with the integrating sphere accessory, by using pressed alumina disk working reflectance references, which had been compared with the NBS SRM 2019A white diffuser in this same equipment. This sphere has a 7° wedge which can be installed at the sample port so that both specular and diffuse components of reflected radiant power can be captured. When the data are corrected for 100-percent reference level and for the absolute reflectance of the alumina, subtraction of the diffuse component from the total (wedge in) yielded the specular component. This equipment yields agreement within 2.5 percent reflectance with the data furnished with an NBS SRM 2021 black diffuser (7–10 percent reflectance levels) in this spectral range.

The FILE instrument filters were mounted in holding fixtures with adjustable apertures to accommodate filters smaller than the sample beam. The aperture was located between the filter and the spectrophotometer detector. The 50- by 50-mm square reference radiometer filters were measured with no aperture masking, since they were much larger than the sampling beam. The transmission measurements on the FILE calibration radiometer filters and the flight-instrument filters, made to define the spectral bandwidths and to determine any changes with time, were made over the 0.625- to 0.675-μm range for the 0.65-μm channel and over the 0.825- to 0.870-μm range for the 0.85-μm channel. The spectrophotometer scan conditions were as follows: 1-second response time, 2-nm spectral slit width, 12 nm/min scan speed, and 0.1-nm sampling interval. Out-of-band transmission is very low, according to the manufacturer's design and specification. (See figs. 2 and 3.) Measurements with the Perkin-Elmer system on the radiometer filters over the 0.2–1.0-μm range detected no out-of-band leakages as large as 0.1 percent transmission. Filter measurements were of specular transmission only.

References

1. Wilson, R. Gale; Sivertson, W. Eugene, Jr.; and Bullock, Gordon F.: Adaptive Remote Sensing Technology for Feature Recognition and Tracking. *1979 IEEE Computer Society Conference on Pattern Recognition and Image Processing*, PR IP 79, c.1978, pp. 623–629.
2. Sivertson, W. E., Jr.; Wilson, R. Gale; Bullock, Gordon F.; and Schappell, R. T.: Feature Identification and Location Experiment. *Science*, vol. 218, no. 4576, Dec. 3, 1982, pp. 1031–1033.
3. Report of WGIRB (Working Group on Infrared Backgrounds): *Infrared Target and Background Radiometric Measurements - Concepts, Units, and Techniques.* 2389-64-T (Contract Nonr 1224(12), Infrared Lab., Univ. of Michigan, Jan. 1962.
4. Nicodemus, Fred E.; and Zissis, George J.: *Methods of Radiometric Calibration.* 4613-20-R (Contract SD-91), Inst. Sci. & Technol., Univ. of Michigan, Oct. 1962.
5. Wyatt, Clair L.: *Radiometric Calibration: Theory and Methods.* Academic Press, Inc., 1978.
6. Turner, Robert E.: *Radiative Transfer in Real Atmospheres.* ERIM 190100-24-T (Contract NAS9-9784), Infrared and Optics Div., Environmental Research Institute of Michigan, July 1974. (Available as NASA CR-140199.)
7. Turner, Robert E.: *Atmospheric Effects in Multispectral Remote Sensor Data.* ERIM 109600-15-F (Contract NAS9-14123), Infrared and Optics Div., Environmental Research Institute of Michigan, May 1975. (Available as NASA CR-141863.)
8. Wolfe, William L.; and Zissis, George J., eds.: *The Infrared Handbook.* Office of Naval Research, Department of the Navy, 1978.
9. Huck, F. O.; Davis, R. E.; Park, S. K.; Aherron, R. M.; and Arduini, R. F.: Computational Modeling for the Study of Multispectral Sensor Systems and Concepts. *Opt. Eng.*, vol. 21, no. 3, May/June 1982, pp. 519–527.
10. Bowker, David E.; Davis, Richard E.; Myrick, David L.; Stacy, Kathryn; and Jones, William T.: *Spectral Reflectances of Natural Targets for Use in Remote Sensing Studies.* NASA RP-1139, 1985.
11. Steven, Michael D.: Standard Distributions of Clear Sky Radiance. *Q. J. R. Meteorol. Soc.*, vol. 103, no. 437, July 1977, pp. 457–465.
12. Sweat, Mark E.; and Carroll, John J.: On the Use of Spectral Radiance Models To Obtain Irradiances on Surfaces of Arbitrary Orientation. *Sol. Energy*, vol. 30, no. 4, 1983, pp. 373–377.
13. Cachorro, V. E.; de Frutos, A. M.; and Casanova, J. L.: Comparison Between Various Models of Solar Spectral Irradiance and Experimental Data. *Appl. Opt.*, vol. 24, no. 19, Oct. 1, 1985, pp. 3249-3253.
14. Nianzeng, Che; Jackson, R. D.; Phillips, A. L.; and Slater, P. N.: The Use of Field Radiometers in Reflectance Factor and Atmospheric Measurements. *Optical Radiation Measurements, Volume 499 of Proceedings of Society of Photo-Optical Instrumentation Engineers*, Aaron A. Sanders, ed., c.1985, pp. 24–33.

Table 1. Spectral Radiance Calibration of Reference Radiometer

Date of measurements	Standard lamp radiance[a] through radiometer bandpass, mW/cm^2-sr		Standard lamp radiance[b] measured by reference radiometer/filter, mW/cm^2-sr		Percentage error in measurements of lamp radiance, percent	
	0.65 μm	0.85 μm	0.65 μm	0.85 μm	0.65 μm	0.85 μm
12/9/83 (preflight)	87.43	145.94	91.11	140.47	4.2	−3.7
12/13/84 (postflight)	87.43	145.94	91.73	140.78	4.9	−3.5

[a]From NBS data.
[b]Corrected for relay lens attenuation; lens transmission was 0.96 at 0.65 μm and 0.97 at 0.85 μm.

Table 2. Earth Feature Reflectance Models Used in Simulations

Wavelength, μm	Reflectance				
	Vegetation	Bare land	Water	Clouds	Average
0.63	0.017	0.240	0.041	0.700	0.250
.64	.014	.247	.041	.700	.251
.65	.010	.250	.040	.700	.250
.66	.010	.258	.039	.699	.252
.67	.011	.260	.034	.698	.251
.83	.308	.309	.010	.690	.329
.84	.307	.308	.010	.690	.329
.85	.305	.309	.010	.689	.328
.86	.306	.311	.011	.689	.329
.87	.308	.315	.011	.639	.331

Table 3. Linearity Verification for CCD Cameras

FILE camera wavelength, μm	Neutral density (ND) filter transmission, percent	FILE response, percent of full scale
0.65	100 (no ND)	100 (no ND)
	82	84
	65	68
	50	52
	24	25
	9	8
.85	100 (no ND)	100 (no ND)
	82	82
	65	64
	50	50
	24	24
	9	8

Table 4. FILE Spectral Responsivity Measurements Before 41-G Flight

Camera band center wavelength, μm	F-number	FILE response, V (percent of full scale)[a]	Reference radiometer measurement, N, $\frac{\text{mW}}{\text{cm}^2\text{-sr-}\mu\text{m}}$	FILE responsivity, R, $\frac{\text{V}}{\text{mW/cm}^2\text{-sr-}\mu\text{m}}$
0.65	5.7	4.8 (96)	29.8	0.16
.85	5.7	4.6 (92)	21.8	.21

[a]Full-scale response was 5 V.

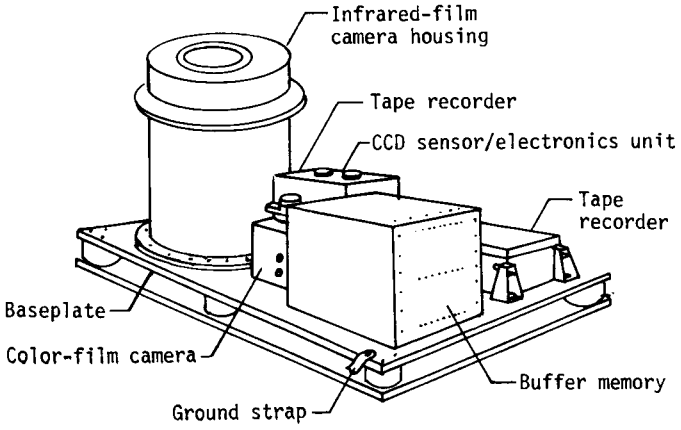

Figure 1. FILE system assembly.

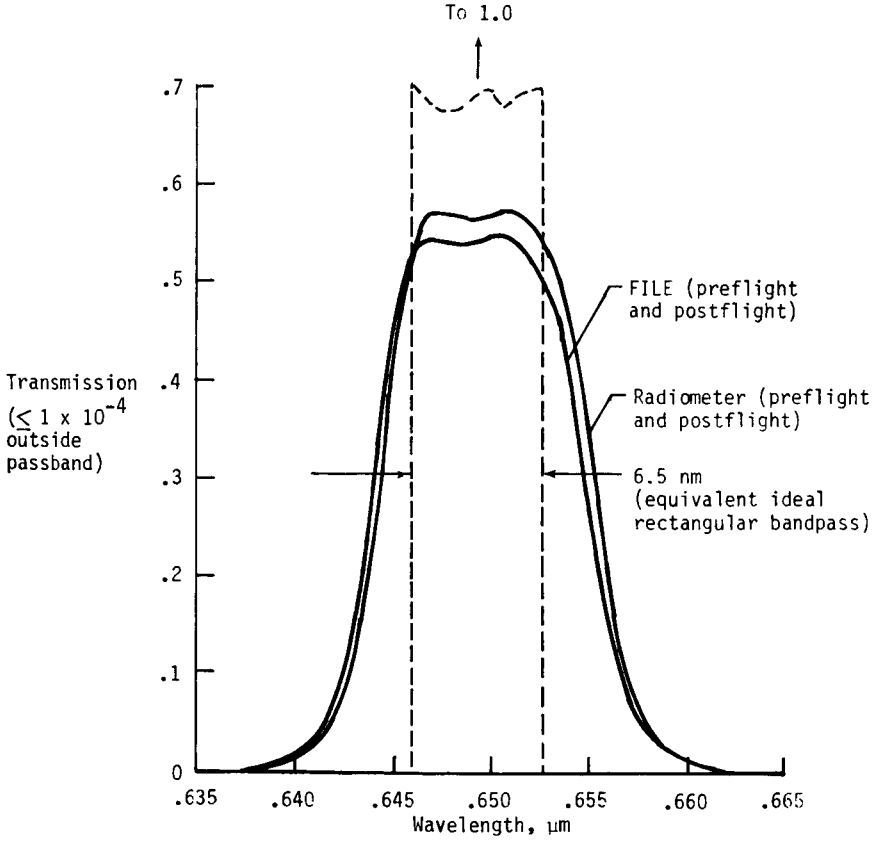

Figure 2. Transmission characteristics of 0.65-μm passband for FILE and reference radiometer instruments.

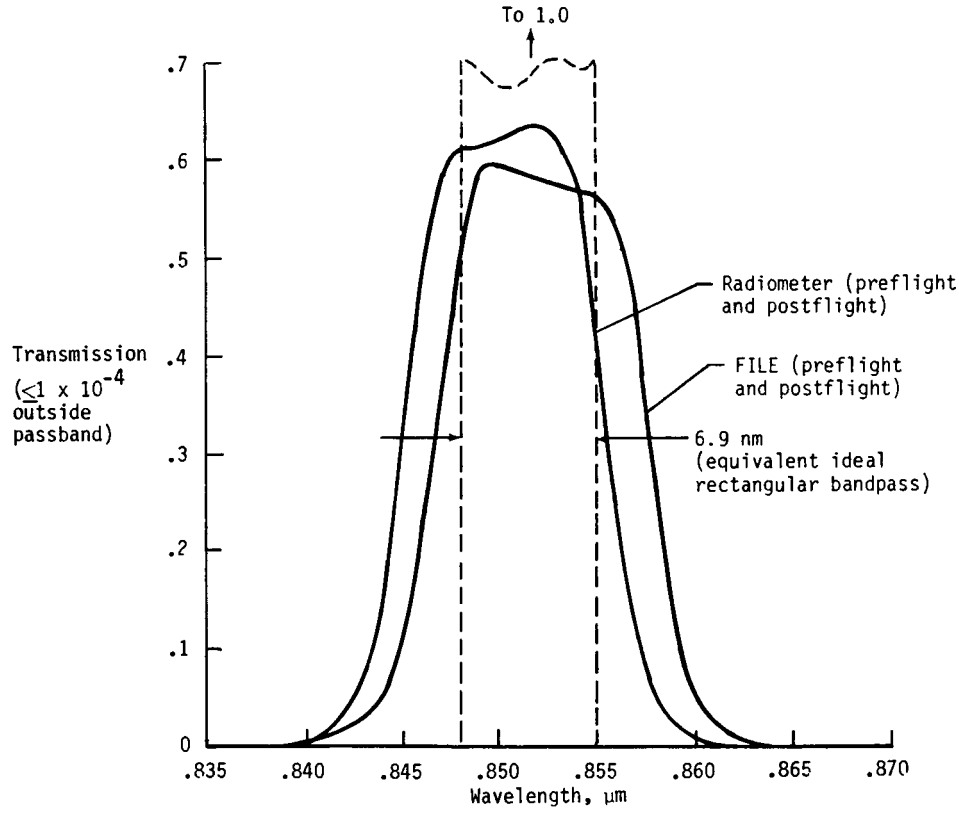

Figure 3. Transmission characteristics of 0.85-μm passband for FILE and reference radiometer instruments.

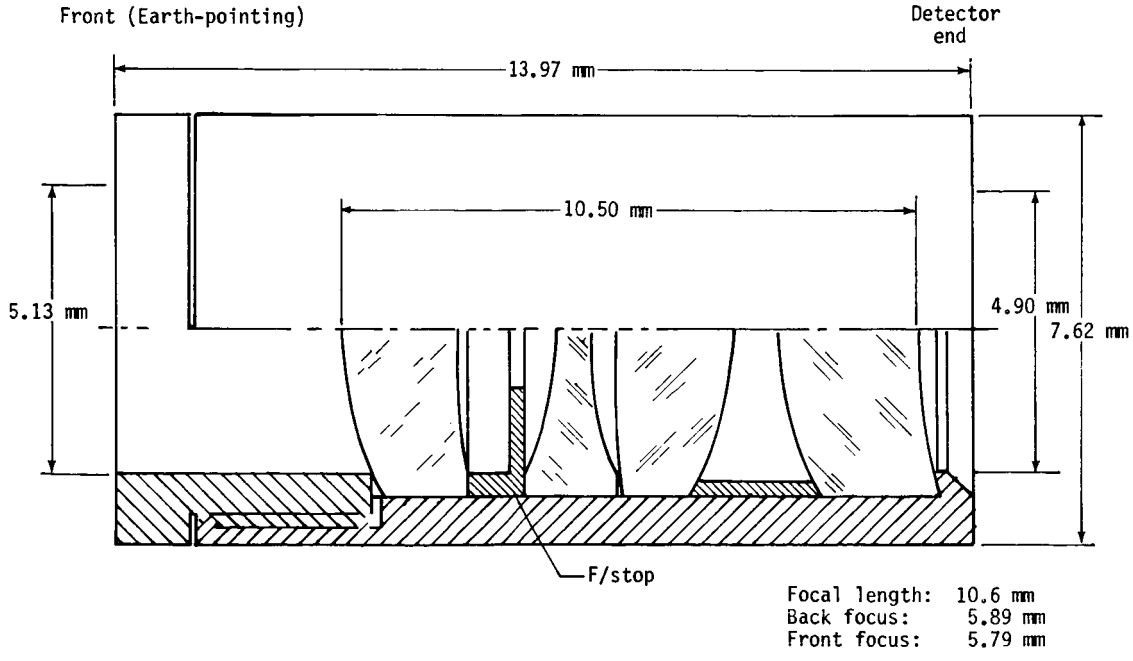

Figure 4. FILE imaging lens.

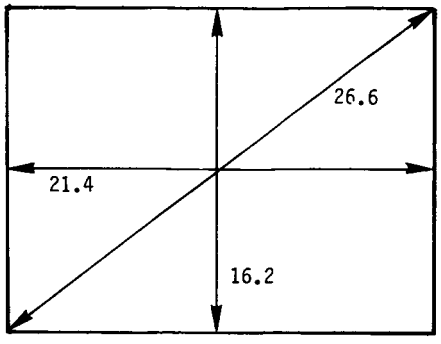

Figure 5. Angular field of view for FILE cameras (in degrees).

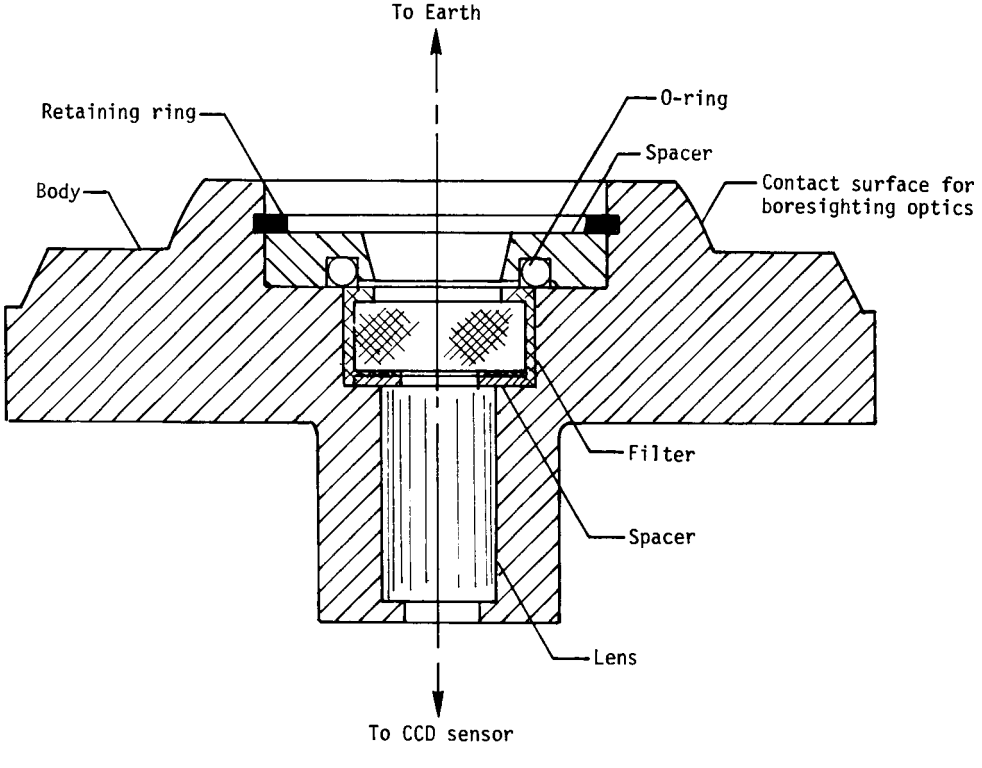

Figure 6. FILE imaging lens-filter assembly.

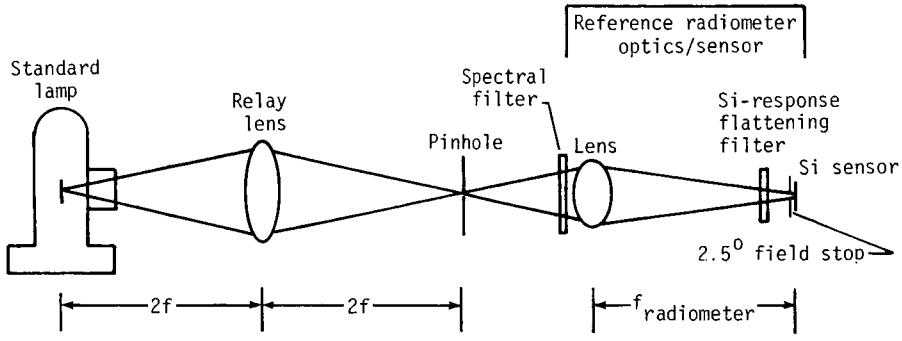

(a) Optics assembly.

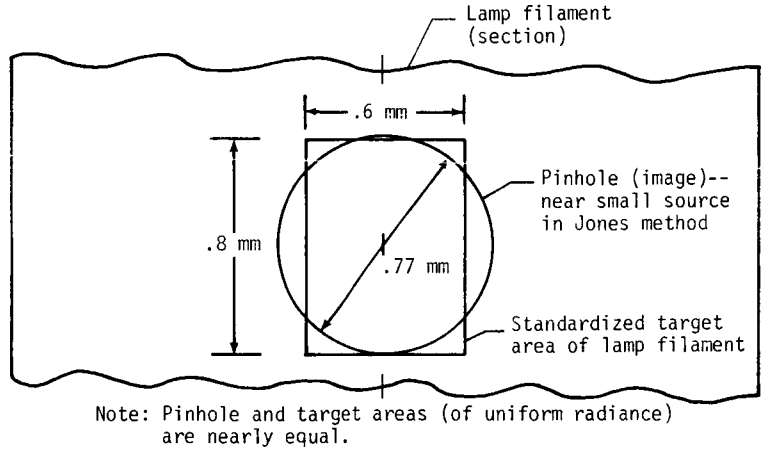

(b) Filament target and pinhole image.

Figure 7. Optical configuration for reference radiometer calibration.

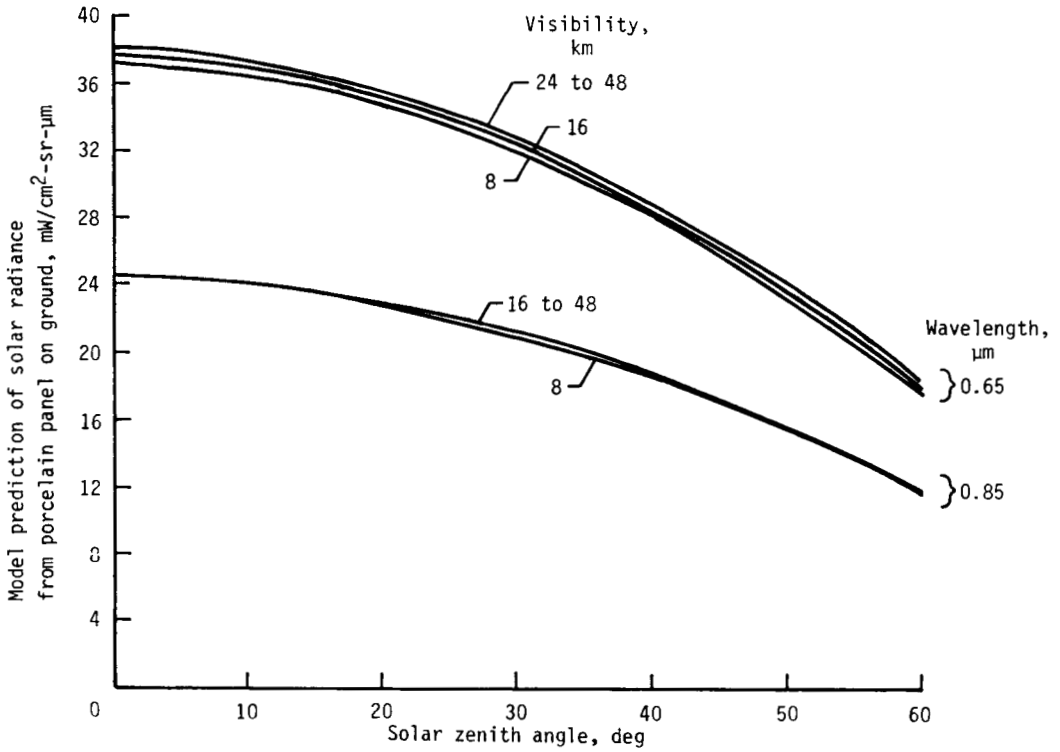

Figure 8. Predicted solar radiance from porcelain reference panel as a function of solar zenith angle, spectral band, and meteorological visibility.

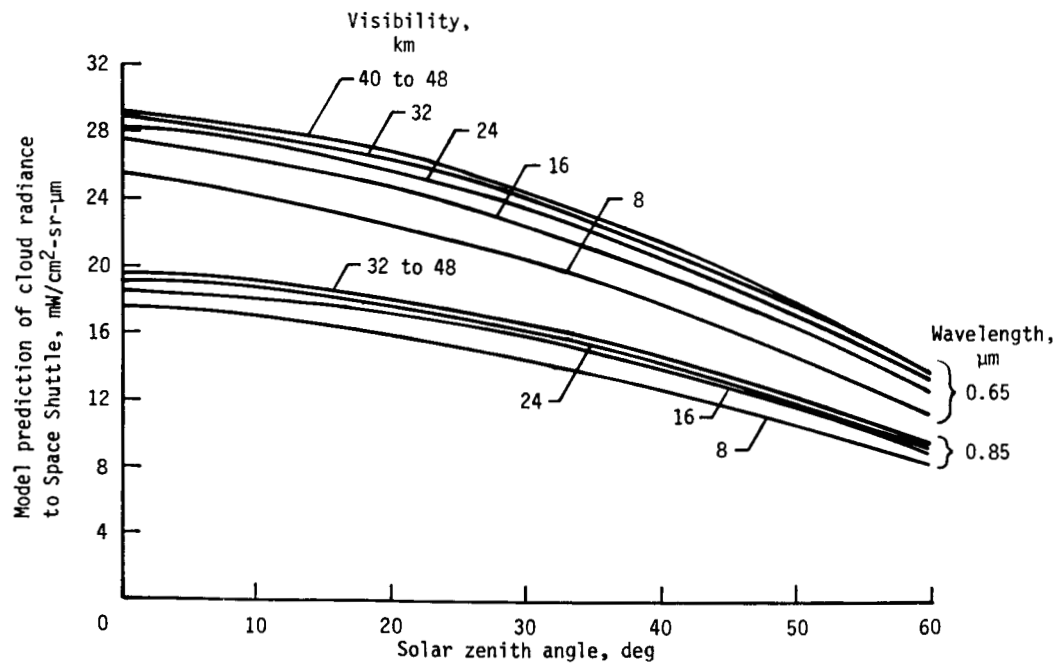

Figure 9. Predicted cloud radiance as a function of solar zenith angle, spectral band, and meteorological visibility.

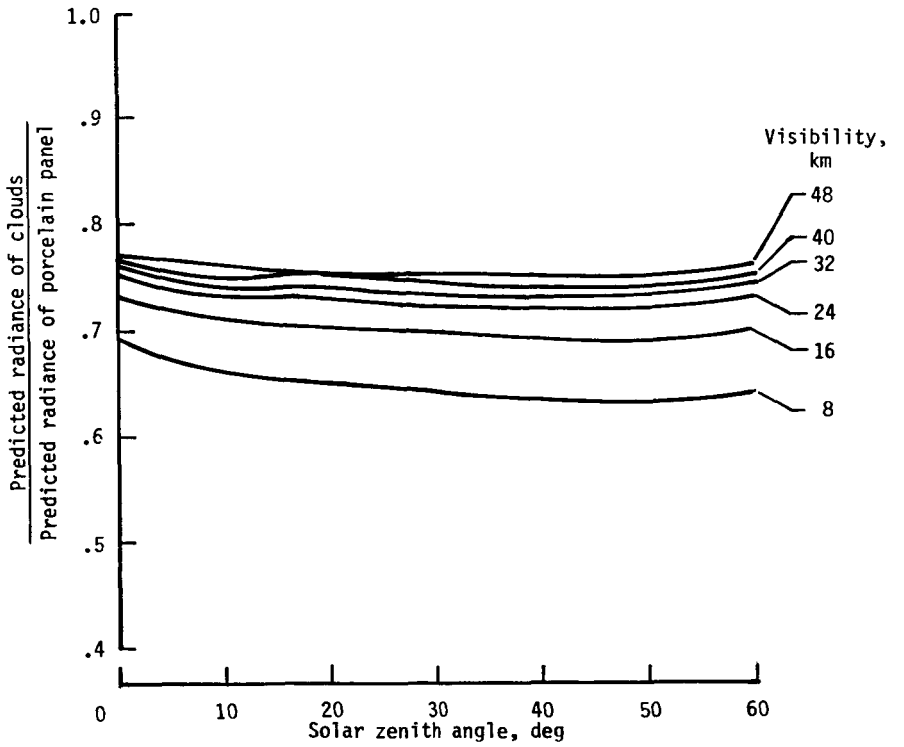

Figure 10. Ratio of predicted cloud radiance (at Space Shuttle) to porcelain panel radiance (on ground) for 0.65-μm channel of FILE instrument.

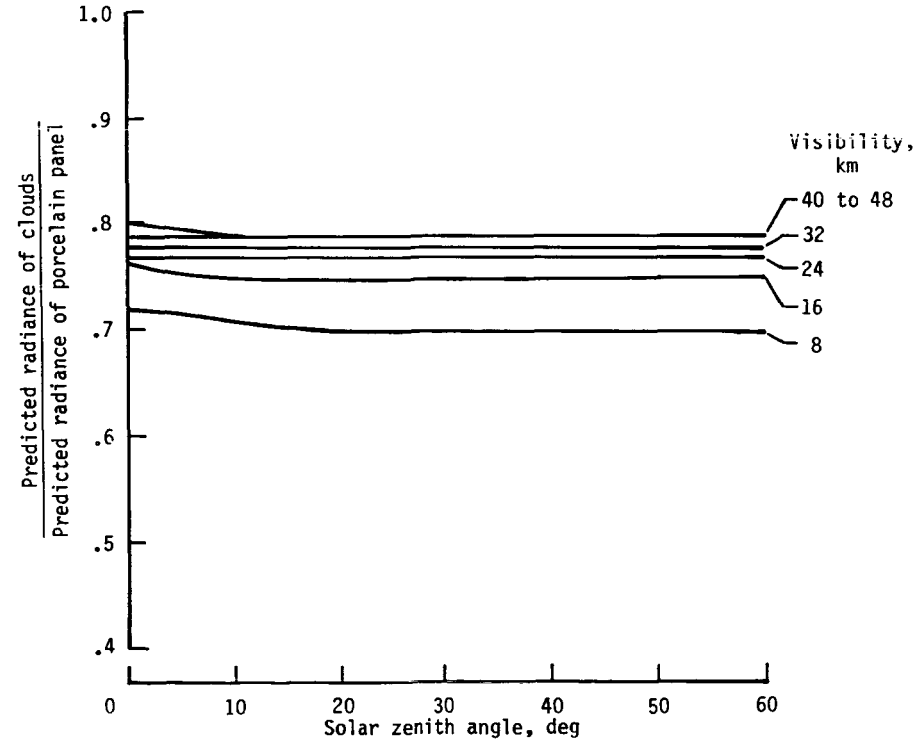

Figure 11. Ratio of predicted cloud radiance (at Space Shuttle) to porcelain panel radiance (on ground) for 0.85-μm channel of FILE instrument.

Standard Bibliographic Page

1. Report No.	2. Government Accession No.	3. Recipient's Catalog No.
NASA TM-89017		

4. Title and Subtitle	5. Report Date
Radiometric Responsivity Determination for Feature Identification and Location Experiment (FILE) Flown on Space Shuttle Mission 41-G	December 1986
	6. Performing Organization Code: 542-03-11-03
7. Author(s): R. Gale Wilson, Richard E. Davis, Robert E. Wright, Jr., W. E. Sivertson, Jr., and Gordon F. Bullock	8. Performing Organization Report No.: L-16180
9. Performing Organization Name and Address: NASA Langley Research Center, Hampton, VA 23665-5225	10. Work Unit No.
	11. Contract or Grant No.
12. Sponsoring Agency Name and Address: National Aeronautics and Space Administration, Washington, DC 20546-0001	13. Type of Report and Period Covered: Technical Memorandum
	14. Sponsoring Agency Code

15. Supplementary Notes

16. Abstract

A procedure was developed to obtain the radiometric (radiance) responsivity of the Feature Identification and Location Experiment (FILE) instrument in preparation for its flight on Space Shuttle Mission 41-G (November 1984). This instrument was designed to obtain Earth feature radiance data in spectral bands centered at 0.65 and 0.85 μm, along with corroborative color and color-infrared photographs, and to collect data to evaluate a technique for in-orbit autonomous classification of the Earth's primary features. The calibration process incorporated both solar radiance measurements and radiative transfer model predictions in estimating expected radiance inputs to the FILE on the Shuttle. The measured data are compared with the model predictions, and the differences observed are discussed. Application of the calibration procedure to the FILE over an 18-month period indicated a constant responsivity characteristic. This report documents the calibration procedure and the associated radiometric measurements and predictions that were part of the instrument preparation for flight.

17. Key Words (Suggested by Authors(s))	18. Distribution Statement
Space Shuttle experiment Feature classification Instrument calibration Solar radiance Radiometry Reflectance Clouds Earth resources Optical instruments Light	Unclassified—Unlimited Subject Category 35

19. Security Classif.(of this report)	20. Security Classif.(of this page)	21. No. of Pages	22. Price
Unclassified	Unclassified	19	A02

For sale by the National Technical Information Service, Springfield, Virginia 22161

NASA-Langley, 1986